Available online at www.sciencedirect.com
SCIENCE DIRECT®
Bioorganic & Medicinal Chemistry Letters 15 (2005) 4057–4063
Bioorganic & Medicinal Chemistry Letters

Molecular recognition of 15-deoxy-$\Delta^{12,14}$-prostaglandin J_2 by nuclear factor-kappa B and other cellular proteins

Vineet Pande and Maria J. Ramos*

REQUIMTE/Departamento de Química, Faculdade de Ciências, Universidade do Porto, Rua do Campo Alegre 687, 4169-007 Porto, Portugal

Received 19 November 2004; revised 1 June 2005; accepted 6 June 2005
Available online 11 July 2005

Abstract—15-Deoxy-$\Delta^{12,14}$-prostaglandin J_2 (15d-PGJ_2), a dehydration product of prostaglandin D_2, is an important pharmacological molecule, which with the virtue of its electrophilicity, has been reported to covalently modify some cellular proteins (such as nuclear factor-kappa B (NF-κB), AP-1, p53, and thioredoxin) and elicit its physiological effects. The aim of the present computational study is to understand the role molecular recognition plays in the association of 15d-PGJ_2 with NF-κB and other proteins. Another aim is to characterize whether p53 is a direct target for covalent modification by 15d-PGJ_2. A docking strategy is applied along with calculation of ab initio electrostatic potential maps to analyze the mode of binding of prostaglandin molecule with critical cysteine-containing sites in each protein. The results provide identification of important sites in the target proteins, which provide recognition and stability to the prostaglandin molecule. Fit of shape and complementarity of electrostatic interactions are derived as significant determinants of molecular recognition of 15d-PGJ_2. Further, comparative results indicate that p53 protein may also be a target for direct modification by 15d-PGJ_2. The molecular models obtained should allow the rational design of more specific analogs of 15d-PGJ_2.

1. Introduction

This study focuses on the understanding of the structural basis of the association of 15-deoxy-$\Delta^{12,14}$-prostaglandin J_2 (15d-PGJ_2) with some of its target proteins, using docking simulations and ab initio electrostatic potential calculations. Prostaglandin D_2 (PGD_2), a major cyclooxygenase product, readily undergoes dehydration in a variety of tissues and cells to yield electrophilic PGs, such as15d-PGJ_2 (Fig. 1).[1]

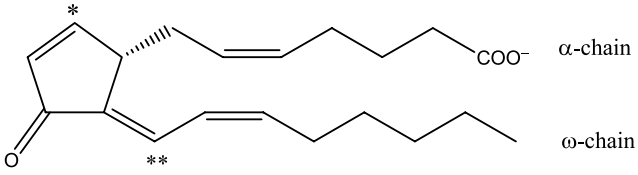

Figure 1. A 15-deoxy-$\Delta^{12,14}$-prostaglandin J_2 molecule depicting the electrophilic carbon (C-9) with an asterisk, and C-13 with double asterisk.

Members of the J series of the PGs, including 15d-PGJ_2, characterized by the presence of a reactive α,β-unsaturated ketone in the cyclopentenone ring (C-9 in Fig. 1, being the biologically active electrophilic carbon), have their own unique spectrum of biological effects, including antitumor activity, the inhibition of cell cycle progression, the suppression of viral replication, the induction of heat shock protein expression, and the stimulation of osteogenesis.[2] Many of these biological effects of 15d-PGJ_2 have been recently attributed to its intervention with some of the cellular proteins. Nuclear factor-kappa B (NF-κB) was described to be one of the first targets of 15d-PGJ_2.[3] NF-κB is a transcription factor that plays a key role in the activation of several inflammatory response genes and its inactivation (especially the p50 subunit) has immense therapeutic implications.[4–6] 15d-PGJ_2 was reported to inhibit multiple steps in the NF-κB signaling pathway[3,7,8] along with specifically inhibiting the NF-κB subunits (p50 and p65), directly by a covalent modification of the subunits.[3,9,10] These studies indicated that 15d-PGJ_2 forms a covalent adduct with the aid of its electrophilic carbon (Fig. 1)

Keywords: 15-Deoxy-$\Delta^{12,14}$-prostaglandin J_2; Molecular recognition; Nuclear factor-kappa B; AP-1; p53; Thioredoxin; Docking; Electrostatic potentials.
* Corresponding author. Tel.: +351 22 60 82 806; fax: +351 22 60 8 2959; e-mail: mjramos@fc.up.pt

0960-894X/$ - see front matter © 2005 Elsevier Ltd. All rights reserved.
doi:10.1016/j.bmcl.2005.06.025

with single critical cysteine residues in the DNA-binding domain of the NF-κB subunits. These critical, redox-regulated cysteine residues are Cys62 in the p50 subunit and Cys38 in the p65 subunit.[11] Further, a reduced state (–SH) of these cysteines has been reported to be essential for DNA recognition and binding, while an oxidized (–S–SR) or alkylated state has been found to diminish DNA-binding of NF-κB.[11–13] Consequently, 15d-PGJ_2 alkylates these nucleophilic cysteine residues.

Recently, the transcription factor AP-1 was reported to be a target of covalent modification of its c-Jun subunit.[14] Similar to NF-κB, AP-1 is a proinflammatory transcription factor and consists of subunits like c-Jun and c-Fos.[15] The redox-regulated critical cysteine residue of AP-1 that modulates its DNA-binding ability is Cys269 in the c-Jun subunit,[16] which is alkylated by 15d-PGJ_2. The role of PGs (especially the A and the J series) in pathological conditions like inflammation and cancer has been described as manifold, as it was reported that 15d-PGJ_2 can inactivate the wildtype p53 tumor-suppressor protein.[17,18] Despite this contrary role, overall activity of 15d-PGJ_2 remains antiproliferative as compared to A-series PGs.[19] The molecular mechanism responsible for p53 inactivation by 15d-PGJ_2 has been proposed to be indirect, unlike NF-κB and AP-1 inhibition. In certain cell types like RKO cells or human neuroblastoma cells, it has been recently proposed that 15d-PGJ_2 inactivates upstream molecules like thioredoxin reductase (TrxR), thioredoxin (Trx),[17] and the proteasome.[18,20] A direct mechanism of action has not been proposed in these cell types, and it has been generalized that 15d-PGJ_2 may interfere with p53 inactivation only indirectly.[17,18,21] However, due to the studies on limited cell types, it has been argued, at the same time, that the indirect mechanism of the action of 15d-PGJ_2 on p53 may be due to specificity issues owing to either the cell type or the p53 protein itself,[14,17] although no structural evidences (like analysis of the mode of binding of the PG to the p53 protein) have been presented in this regard. Further, Trx, upstream of p53 pathway, has been proposed to be a target of direct covalent modification at its active-site cysteine (Cys35), by 15d-PGJ_2.[20]

In general, since 15d-PGJ_2 is a weak electrophile, its selectivity for the target proteins, and for instance not with DNA, and other susceptible proteins like PPAR-γ (DNA-binding domain) has been experimentally described as being possibly controlled by molecular recognition;[3,14,22] however, no molecular models of the complexes have yet been presented. The purpose of the present computational study is to use the available experimental information on the inhibition of cellular proteins by 15d-PGJ_2 to model its molecular recognition and structural association with them. In addition, in case of NF-κB (p50), and AP-1 (c-jun), covalent modification of the critical cysteine residues mentioned above by glutathione has been described to be well correlated with molecular recognition.[16,23] Further, molecular recognition has been recently exploited to achieve specific covalent modification of p50-Cys62 by a NF-κB decoy hairpin oligonucleotide.[24]

With the availability of biochemical knowledge of the present system, an understanding of the docking sites in the target proteins, providing stabilization to the PG molecule, and physiochemical nature of such stabilization should be an additional advantage for further studies. Such an understanding, which is the purpose of this study, would aid in initiating rational design of analogs having NF-κB-specific recognition. This is significant in terms of pharmacological interventions using 15d-PGJ_2, as the concentrations of 15d-PGJ_2 used to achieve NF-κB inhibition in inflammatory models are relatively quite high.[25] The protein targets used in this study, including NF-κB (p50 and p65 subunits), AP-1 (c-Jun subunit), and Trx, all have experimentally studied cysteine residues, targeted for covalent modification by 15d-PGJ_2. It is well known that p53 also has a redox-regulated cysteine (Cys277) in its DNA-binding domain, which is quite identical to NF-κB and AP-1, in terms of its pK_a value and control of DNA recognition and binding.[26–28] Hence, we hypothesized that under identical conditions this cysteine may also be a target of direct modification by 15d-PGJ_2, and used it to model the molecular recognition.

2. Results and discussion

2.1. Docking studies

The 15d-PGJ_2 molecule was subject to docking with the proteins p50, p65, c-Jun, Trx, and p53 to predict the possible structural interactions in the process of the molecular recognition and stabilization of the molecule by the proteins. The docking approach employed here is justified in certain ways to produce realistic binding modes of 15d-PGJ_2 with its target proteins. First, the ChemScore function used here includes a lipophilic term that is very useful in docking ligands (like 15d-PGJ_2) with hydrophobic character. Further, in the initial ChemScore training set, some of the protein–ligand complexes were very similar to the present system, for example, the flexible palmitic acid–FABP complex.[41] In addition, in a recent study of some tea polyphenols, covalently modifying a target threonine residue in the proteasome, a distance constraint approach, like the one used in this work, was employed using the AutoDock docking program to understand the nature of pre-covalent complexes.[29] With such a distance constraint approach, the conformational search space around a predefined binding site for a small ligand is much reduced due to partial knowledge of the binding mode, resulting in more reliable models.[29,39] Figures. 2a–e depicts the best scored results given by GOLD. Non-covalent interactions are discussed below.

2.1.1. Hydrogen-bonding interactions. All the five proteins used in this study were found to make strong hydrogen-bonding interactions with the carboxyl group of 15d-PGJ_2. Proteins p50, p65, and c-Jun make strong hydrogen bonds (<2 Å) through lysine residues (Figs. 2a, b, e) and p53 through an arginine residue (Fig. 2c). Further, Trx was observed to make a hydrogen bond through the backbone (—NH) hydrogen atom of

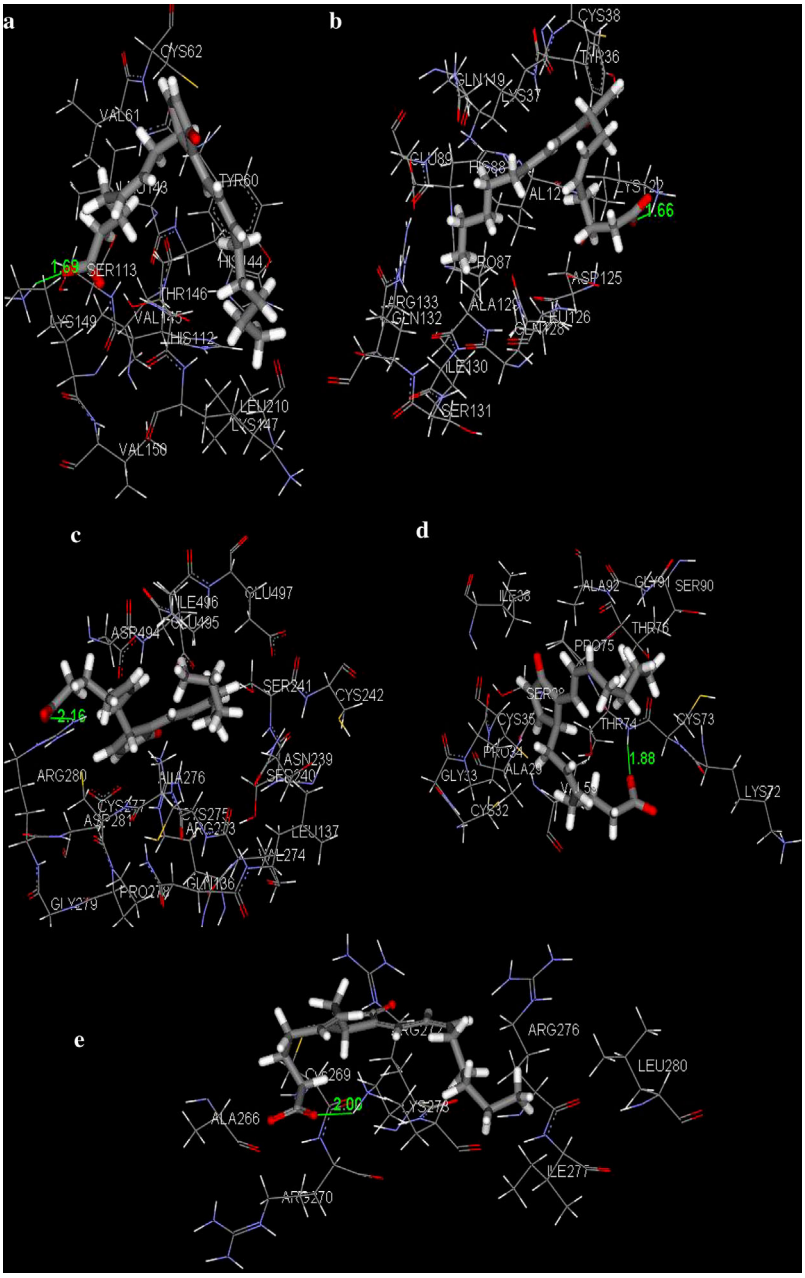

Figure 2. 15d-PGJ_2 is shown docked to the target proteins: (a) p50, (b) p65, (c) p53, (d) Trx, and (e) c-Jun. Nitrogen atoms are depicted in blue, oxygen atoms in red, hydrogens in white, and sulfur atoms in yellow. Hydrogen-bonding interactions (in angstroms) are depicted in green lines.

Thr74 residue. It is important to note here that a specific hydrogen-bonding interaction with the carboxy-terminal part of the α-chain has been experimentally described as an important determinant of specific molecular recognition of PG-like fatty acids with their natural receptors.[30,31] Analogously, 15d-PGJ_2 may be recognizing its target proteins through the predicted hydrogen-bonding interactions.

2.1.2. Hydrophobic and van der Waals interactions. The remaining nonpolar part of the α-chain and the completely nonpolar ω-chain of 15d-PGJ_2 were also found to recognize the target proteins and stabilize the molecule through hydrophobic and van der Waals interactions (Fig. 2). Specifically, p50 has residues around Cys62 like Val145, Leu143, and Leu210, which were found to stabilize the PG molecule (Fig. 2a) with hydrophobic interactions, besides residues like His144 and Lys147, making van der Waals interactions. Similarly, p65 also has Val121 and Ala129 residues providing hydrophobic interactions mainly with the ω-chain. The α-chain in the case of p65 can be seen as bent in order to interact through a hydrogen bond with Lys122 (Fig. 2b) to avoid opposite interactions with negatively charged Asp125, which lies in the vicinity. Further, in the case of p53, the probable target cysteine, Cys277 (which lies in the solvent accessible surface), is also surrounded by hydrophobic residues like Ile496, Ala276,

and Leu137 (Fig. 2c), providing stabilization to the nonpolar parts of the PG molecule.

Next, in the case of c-Jun, an excellent correlation with the recent experimental results[14] was observed. The nonpolar parts of 15d-PGJ_2 are stabilized by van der Waals and hydrophobic interactions with Arg270, Leu280, and Ile277 residues of c-Jun (Fig. 2d). However, the C-13 containing part of the ω-chain (Fig. 1), remains not much incorporated into the protein (Fig. 2d). This may be true due to some reasons. First, c-Jun is an elongated, linear protein, so that the ligands binding to its residues, for instance Cys269, might eventually have a significant part unembedded. Secondly, in the case of 15d-PGJ_2, there is another electrophilic carbon, C-13, other than the more significant one in the ring, which was experimentally observed to cross-link two c-Jun molecules, in the process of the inhibition of c-Jun–DNA binding.[14] Hence, the net orientation of 15d-PGJ_2 molecule in the present docking, resulting in a relatively free C-13, should be available for another nucleophilic attack by a c-Jun monomer. Finally, in the case of Trx, the nonpolar part of α-chain is stabilized by interactions with Ala29 and Pro34, and the ω-chain by interactions with Ala92, Pro75, and Ile38 (Fig. 2e).

2.2. Molecular electrostatic potentials

Besides hydrogen-bonding and van der Waals interactions, the net electrostatic potential that is created in the space around a molecule by its nuclei and electrons has been proven to be very useful in explaining both long-range molecular recognition and short-range intermolecular stabilization.[32] Theoretically calculated MEPs using QM-derived electron density have been described to be very predictive of the mode of molecular recognition.[33] The electron density calculation approach used in the present study has been recently reported by us for different biological systems including NF-κB[34–37] and has given results in good agreement with the experiment. In the present case, the QM calculations were used to obtain the precise electron density around the PG molecule and each target protein part representing sufficient size in terms of docked molecule. The MEPs mapped on the solvent-accessible surfaces of 15d-PGJ_2 and the inhibitor-interacting parts of the five target proteins are shown in Figures 3a–f. In Figures 3b–f, the PG molecule is aligned onto the solvent-accessible surface of each protein in the same orientation as given by the highest scored docking result. These color-coded surfaces represent a positive potential in blue and a negative potential in red color. The electronic properties of 15d-PGJ_2 molecule are revealed in its MEP surface (Fig. 3a), as its α-chain, containing the nonconjugated double bond and the carboxylate end render itself in electronegative potential, while its ω-chain having a cross-conjugation with the cyclopentenone moiety is rendered in a net electropositive potential. Further, it is observed that the orientation and association of the prostaglandin molecule obtained by docking with each protein is quite in agreement with the electrostatic profile of interactions (Figs. 3b–f). Specifically, with p50, 15d-PGJ_2 fits itself in complementary pockets (Fig. 3b), and with p65, the trends discussed in docking are again revealed, as the α-chain recognizes the electropositive part and bends upward to avoid interaction with electronegative part in the bottom vicinity (Fig. 3c). Next, in the case of Trx and c-Jun, the α-chain resides in complementary surfaces, although the ω-chain lies in more neutral surfaces (Figs. 3d–f). This is justified for c-Jun, as the ω-chain is not so well stabilized by the protein electrostatics, to cross-link with another c-Jun molecule. Further, in the case of p53, the ω-chain stabilizes in a neutral-hydrophobic pocket, having an orientation toward electronegative parts, as also in the case of Trx (Figs. 3d and e).

3. Conclusions

The docking studies in combination with comparative electrostatic potentials reveal that 15d-PGJ_2 has complementary interactions with its target proteins, governed mainly by fit of shape (hydrophobic and van der Waals interactions) in all the cases and also complementarity of electrostatics. These results thus support the experimental assertion of the possible role of molecular recognition of 15d-PGJ_2 by cellular proteins[3,14,22] Especially, in the case of NF-κB p50, important binding pockets are revealed and provide specific recognition and stabilization to the prostaglandin molecule. The protein environment in terms of hydrophobic pockets or electrostatic and hydrogen-bonding interactions, not known previously and revealed in the present study, should be an important determinant of the molecular recognition of 15d-PGJ_2. An important implication of this study is that the incorporation of 15d-PGJ_2 with its cellular targets is not a random process. Further, the knowledge of the complementary binding sites should provide a guideline for the design of specific and efficient inhibitors of transcription,[4,6] structurally based on 15d-PGJ_2.

Another indication of this comparative study is the fact that the association of 15d-PGJ_2 with p53 is also complementary under identical conditions, just as with the other target proteins, and hence the possibility of p53 being a target for direct modification cannot be excluded. It is quite clear with the present results that the experimentally observed indirect activity of 15d-PGJ_2 for p53 might concern specificity issues pertaining to cell type rather than protein itself, as discussed in recent studies.[14,17] Hence, further experimental studies in different cell types are required; also important will be the exploration of possible cell-surface receptors of 15d-PGJ_2, as they might be controlling its intracellular concentrations in in vitro models.

4. Materials and methods

4.1. Models

All the protein structures were obtained from Protein Data Bank (PDB IDs for p50 and p65: 1vkx, p53: 1ycs, c-Jun: 1a02, and Trx: 3trx), and individual subunits were further managed with Insight II molecular

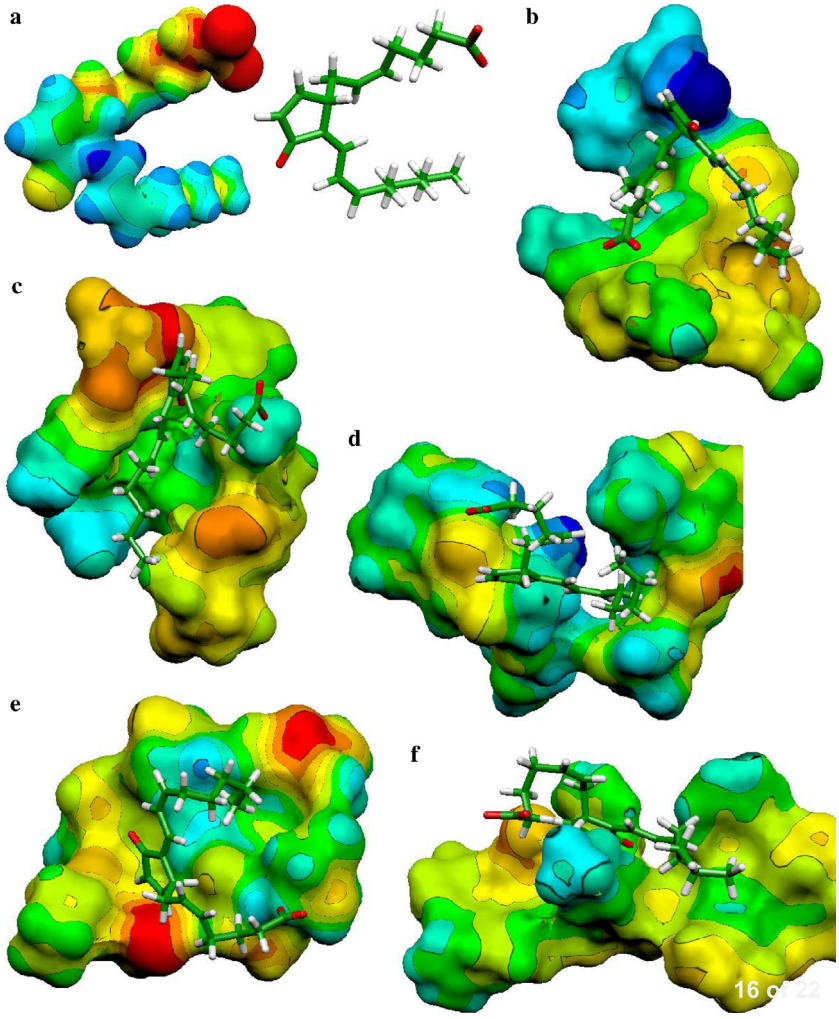

Figure 3. Molecular electrostatic potentials (MEPs) are shown mapped onto the solvent-accessible surfaces of each structure, with maximum potential (blue) being $\phi_+ = 0.5102$ au, and the minimum (red) being $\phi_- = -0.3188$ au. (a) Structure of 15d-PGJ_2 is shown along with its MEP. (b)–(f) represent the prostaglandin molecule docked onto the electrostatic potential surfaces of p50, p65, p53, Trx, and c-Jun, respectively.

modeling system (Accelrys Inc., San Diego, CA, USA). The target cysteine in each protein molecule was modeled as a nucleophilic thiolate, as the reaction with 15d-PGJ_2 has been proposed to occur when first the cysteine has a free sulfur atom for attack.[1] Further, 15d-PGJ_2 was energy minimized using density functional theory with the B3LYP functional and 6-31+G(d) basis set in Gaussian 98 package.[38]

4.2. Docking studies

Docking studies were performed using the GOLD 2.0 package (CCDC Software Ltd, Cambridge, UK).[39,40] To simulate the formation of the precovalent complexes and to interpret the possible sites in the proteins which might stabilize and accommodate the PG molecule, the following strategy was used. An initial distance constraint of 2 Å was imposed between the C-9 atom of 15d-PGJ_2 molecule and the target thiolate group of each protein, and the PG was allowed to freely dock in an energetically and conformationally best orientation. Docking simulations were performed in the default settings for the best possible predictive accuracy, with 10 docking runs for each protein. Hydrogen bonds were considered up to 2.5 Å. GOLD uses a genetic algorithm in the evolution of a population of possible solutions via genetic operators (mutations, crossovers, and migrations) to a final population, optimizing a predefined fitness function. The predefined function used in this study is implemented in GOLD in the form of ChemScore.[41,42] Briefly, ChemScore estimates the total free-energy change that occurs on ligand binding as

$$\Delta G_{\text{binding}} = \Delta G_0 + \Delta G_{\text{hbond}} + \Delta G_{\text{metal}} + \Delta G_{\text{lipo}} + \Delta G_{\text{rot}}.$$

Each component of this equation is the product of a term dependent on the magnitude of a particular physical contribution to free energy (hbond = hydrogen bond, lipo = lipophilic atoms, and rot = rotable bonds) and a scale factor determined by regression,

$$\Delta G_0 = v_0, \quad \Delta G_{\text{hbond}} = v_1 P_{\text{hbond}}, \quad \Delta G_{\text{metal}} = v_2 P_{\text{metal}},$$
$$\Delta G_{\text{lipo}} = v_3 P_{\text{lipo}}, \quad \Delta G_{\text{rot}} = v_4 P_{\text{rot}}.$$

Here, v is the regression coefficient and P the various types of physical contributions to binding. The final ChemScore value is obtained by adding in a clash penalty and internal torsion terms, which militate against close contacts in docking and poor internal conformations. In the present study, as mentioned before, a constraint score was also included:

$$\text{ChemScore}_{(\text{this study})} = \Delta G_{\text{binding}} + P_{\text{clash}} + P_{\text{internal}} + P_{\text{constraint}}.$$

The best scored solution in each case was considered and analyzed in DS ViewerPro 5.0 modeling package (Accelrys Inc.).

4.3. Molecular electrostatic potentials

To analyze the extent of agreement between the fit obtained by docking and complementarity in the electrostatics of binding, ab initio electrostatic potential maps were generated for the PG molecule and the interactive part of each target protein. Each protein was cut at 6 Å radii around the PG molecule obtained from the highest scored docking solution, representing enough amino acids in the protein site contributing to electrostatic interactions. Ab initio quantum-mechanical (QM) calculations were performed with the B3LYP functional and 6-31+G(d) basis set in Gaussian 98 program.[38] The electron density thus obtained for each protein cut and the PG molecule was further used to generate molecular electrostatic potential (MEP) maps, representing the relative population of charges, graphically. MOLEKEL 4.2[43] was used to generate solvent-accessible Connolly surfaces, with a probe radius of 1.4 Å,[44] and the calculated electrostatic potential was mapped onto these surfaces. The maximum potential represented is $\phi_+ = 0.5102$ au and the minimum is $\phi_- = -0.3188$ au for each surface depicted. Other ranges of potentials gave virtually the same results.

Acknowledgments

We thank the NFCR Centre for Computational Drug Discovery, University of Oxford, UK for Ph.D. scholarship to V.P. and FCT, Portugal for financial support.

References and notes

1. Straus, D. S.; Glass, C. K. *Med. Res. Rev.* **2001**, *21*, 185.
2. Soberman, R. J.; Christmas, P. *J. Clin. Invest.* **2003**, *111*, 1107.
3. Straus, D. S.; Pascual, G.; Li, M.; Welch, J. S.; Ricote, M.; Hsiang, C.-H.; Sengchanthalangsy, L. L.; Ghosh, G.; Glass, C. K. *Proc. Natl. Acad. Sci. U.S.A.* **2000**, *97*, 4844.
4. Pande, V.; Ramos, M. J. *Curr. Med. Chem.* **2003**, *10*, 1603.
5. Karin, M.; Yamamoto, Y.; Wang, Q. M. *Nat. Rev. Drug Discov.* **2004**, *3*, 17.
6. Pande, V.; Ramos, M. J. *Curr. Med. Chem.* **2005**, *12*, 357.
7. Rossi, A.; Kapahi, P.; Natoli, G.; Takahashi, T.; Chen, Y.; Karin, M.; Santoro, M. G. *Nature* **2000**, *403*, 103.
8. Castrillo, A.; Díaz-Guerra, M. J. M.; Hortelano, S.; Martín-Sanz, P.; Boscá, L. *Mol. Cell. Biol.* **2000**, *20*, 1692.
9. Cernuda-Morollón, E.; Pineda-Molina, E.; Cañada, F. J.; Pérez-Sala, D. *J. Biol. Chem.* **2001**, *276*, 35530.
10. Pérez-Sala, D.; Cernuda-Morollón, E.; Pineda-Molina, E.; Cañada, F. J. *Ann. N.Y. Acad. Sci.* **2002**, *973*, 533.
11. Kumar, S.; Rabson, A. B.; Gelinas, C. *Mol. Cell. Biol.* **1992**, *12*, 3094.
12. Matthews, J. R.; Kaszubska, W.; Turcatti, G.; Wells, T. N.; Hay, R. T. *Nucleic Acids Res.* **1993**, *21*, 1727.
13. Christman, J. W.; Blackwell, T. S.; Juurlink, B. H. J. *Brain Pathol.* **2000**, *10*, 153.
14. Pérez-Sala, D.; Cernuda-Morollón, E.; Cañada, F. J. *J. Biol. Chem.* **2003**, *278*, 51251.
15. Karin, M. *J. Biol. Chem.* **1995**, *270*, 16483.
16. Klatt, P.; Pineda-Molina, E.; De Lacoba, M. G.; Padilla, C. A.; Martinez-Galisteo, E.; Bárcena, J. A.; Lamas, S. *FASEB J.* **1999**, *13*, 1481.
17. Moos, P. J.; Edes, K.; Cassidy, P.; Massuda, E.; Fitzpatrick, F. A. *J. Biol. Chem.* **2003**, *278*, 745.
18. Shibata, T.; Yamada, T.; Kondo, M.; Tanahashi, N.; Tanaka, K.; Nakamura, H.; Masutani, H.; Yodoi, J.; Uchida, K. *Biochemistry* **2003**, *42*, 13960.
19. Moos, P. J.; Edes, K.; Fitzpatrick, F. A. *Proc. Natl. Acad. Sci. U.S.A.* **2000**, *97*, 9215.
20. Shibata, T.; Yamada, T.; Ishii, T.; Kumazawa, S.; Nakamura, H.; Masutani, H.; Yodoi, J.; Uchida, K. *J. Biol. Chem.* **2003**, *278*, 26046.
21. Mullally, J. E.; Moss, P. J.; Edes, K.; Fitzpatrick, F. A. *J. Biol. Chem.* **2001**, *276*, 30366.
22. Fukushima, M. *Eiconasoids* **1990**, *3*, 189.
23. Pineda-Molina, E.; Klatt, P.; Vázquez, J.; Marina, A.; Lacoba, M. G.; Pérez-Sala, D.; Lamas, S. *Biochemistry* **2000**, *40*, 14134.
24. Lesage, D.; Metelev, V.; Borisova, O.; Dolinnaya, N.; Oretskaya, T.; Baran-Marszak, F.; Taillandier, E.; Raphael, M.; Fagard, R. *FEBS Lett.* **2003**, *547*, 115.
25. Bureau, F.; Desmet, C.; Mélotte, D.; Jaspar, F.; Volanti, C.; Vanderplasschen, A.; Pastoret, P.-P.; Piette, J.; Lekeux, P. *J. Immunol.* **2002**, *168*, 5318.
26. Hainaut, P.; Milner, J. *Cancer Res.* **1993**, *53*, 4469.
27. Buzek, J.; Latonen, L.; Kurki, S.; Peltonen, K.; Laiho, M. *Nucl. Acids Res.* **2002**, *30*, 2340.
28. Wu, H.-H.; Sherman, M.; Yuan, Y.-C.; Momand, J. *Gene Ther. Mol. Biol.* **1999**, *4*, 119.
29. Smith, D. M.; Daniel, K. G.; Wang, Z.; Guida, W. C.; Chan, T.-H.; Dou, Q. P. *Proteins* **2004**, *54*, 58.
30. Nolte, R. T.; Wisley, G. B.; Westin, S.; Cobb, J. E.; Lambert, M. H.; Kurokawa, R.; Rosenfeld, M. G.; Willson, T.; Glass, C. K.; Milburn, M. V. *Nature* **1998**, *395*, 137.
31. Xu, H. E.; Lambert, M. H.; Montana, V. G.; Parks, D. J.; Blanchard, S. G.; Brown, P. J.; Sternbach, D. D.; Lehmann, J. M.; Wisley, G. B.; Willson, T. M.; Kliewer, S. A.; Milburn, M. V. *Mol. Cell.* **1999**, *3*, 397.
32. Murray, J. S.. In Kollman, P. A., Allinger, N., Eds.; The Encyclopedia of Computational Chemistry; John Wiley and Sons: Chichester, UK, 1998.
33. Exner, T. E.; Mezey, P. G. *J. Phys. Chem. A.* **2002**, *106*, 11791.
34. Pande, V.; Sharma, R. K.; Inoue, J.-I.; Otsuka, M.; Ramos, M. J. *J. Comput. Aided Mol. Des.* **2003**, *17*, 825.
35. Portela, C.; Afonso, C. M.; Pinto, M. M.; Ramos, M. J. *FEBS Lett.* **2003**, *17*, 217.
36. Portela, C.; Afonso, C. M.; Pinto, M. M.; Ramos, M. J. *Bioorg. Med. Chem.* **2004**, *12*, 3313.
37. Sharma, R. K.; Otsuka, M.; Pande, V.; Inoue, J.-I.; Ramos, M. J. *Bioorg. Med. Chem. Lett.* **2004**, *14*, 6123.
38. Frisch, M. J.; Trucks, G. W.; Schlegel, H. B.; Scuseria, G. E.; Robb, M. A., et al. GAUSSIAN 98 (Revision A1), Gaussian, Pittsburgh, PA, 1998.
39. Jones, G.; Willett, P.; Glen, R. C. *J. Mol. Biol.* **1995**, *245*, 43.

40. Jones, G.; Willett, P.; Glen, R. C.; Leach, A. R.; Taylor, R. *J. Mol. Biol.* **1997**, *267*, 727.
41. Eldridge, M. D.; Murray, C. W.; Auton, T. R.; Paolini, G. V.; Mee, R. P. *J. Comput. Aided Mol. Des.* **1997**, *1*, 425.
42. Baxter, C. A.; Murray, C. W.; Clark, D. E.; Westhead, D. R.; Eldridge, M. D. *Proteins* **1998**, *33*, 367.
43. Portmann, S.; Lüthi, P. *Chimia* **2000**, *54*, 766.
44. Connolly, M. L. *Science* **1983**, *221*, 709.